PROCEEDINGS OF SCIENCE

Lead shielding impact on fast neutron spectrum (>10 MeV) in QUINTA uranium

M. Szuta[1], **E. Strugalska-Gola, S. Kilim, M. Bielewicz**
National Centre for Nuclear Research NCBJ
05-400 Otwock-Świerk, Polandy
E-mail:Marcin.Szuta@ncbj.gov.pl, Elzbieta Strugalska-Gola@ncbj.gov.pl , Stanislaw.Kilim@ncbj.gov.pl, Marcin.Bielewicz@ncbj.gov.pl

S. Tyutyunnikov
Joint Institute for Nuclear Research
Joliot Curie str.Dubna Moscow region14198 Russia
E-mail:Tsi@sunse.jin.rul

V. Chilap
Center Physical and Technical Projects "Atomenergomash"
Klara Cetkin str. 33, Moscow, 125130 Russia
E-mail:Stanislaw.Kilim@ncbj.gov.pl

The QUINTA uranium target is a deeply sub-critical active core consisting of 512 kg of natural uranium rods arranged hexagonally. The target is irradiated by a pulsed beam of relativistic ions using the JINR NUCLOTRON accelerator. In the paper the lead shielding impact on fast neutron spectrum in the QUINTA uranium target is studied. The fast neutron energy spectra inside the volume of the QUINTA uranium target using threshold reaction in natural yttrium (^{89}Y) were measured for the same deuteron energy of 4 GeV when the uranium target of the assembly was enfolded with the lead shielding and without the shielding. The (n,xn) reaction rates of yttrium samples located inside the assembly were determined through gamma spectrometry. The measurement show that the neutron flux density increases in whole volume of the QUINTA assembly due to the lead shielding. The lead shielding influence on the neutron spectra is more pronounced in the volume located closer to the shielding. Here you can write the abstract for your paper.

XXII International Baldin Seminar on High Energy Physics Problems
JINR, Dubna, Russia
September 15-20, 2014

[1] Speaker

PoS(Baldin ISHEPP XXII)060

1. Introduction

The physical aspects of electronuclear energy production are actively studied today in many scientific centers all over the world.

Most activities are concentrated on the classical electronuclear systems - Accelerator Driven Systems (ADS) - based on spallation neutron generation, with a spectrum harder than that of fission neutrons, by protons with an energy of about 1 GeV in a high-*Z* target. These neutrons can also be used for generation of nuclear energy in the active zone having criticality of 0.94 - 0.98 and surrounding the target.

Study of deep subcritical electronuclear systems and feasibility of their application for energy production and radioactive waste transmutation using relativistic beams from the JINR Nuclotron, which we are involved in, is performed within the E&T RAW collaboration. This work is a preliminary step toward the study of the physical properties of ADS systems, in which a deeply subcritical active core (AC) from natural uranium is irradiated by a pulsed beam of relativistic deuterons. The long-range goal is the study of the possibilities of such systems with maximally hard neutron spectrum, to carry out transmutation of RAW, and also to gain energy due to burning of AC material.

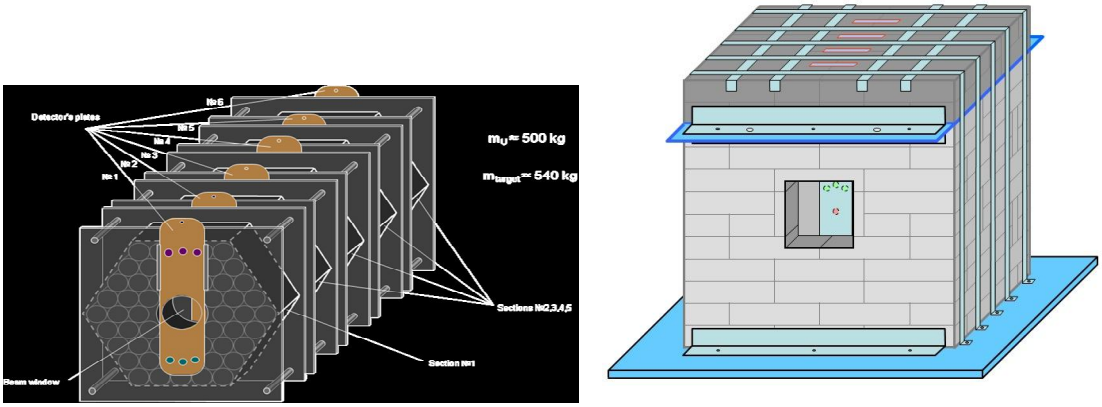

Figure 1. Schema of Quinta assembly. On the left there is a view on the uranium target with supporting structures and plastics used for sample placement (detector's plates), on the right there is a view on the lead shielding enfolding the target.

The scientific program of the project includes activities in four basic directions: integral data, constants, simulation and materials which represent a complex of self-consistent mutually complementary experiments, together with numerical and theoretical studies [1].

We have started with experiments which refer to the study of neutron spectra at various points in the volume of the assembly QUINTA (see Fig. 1.). These are the first experiments with a set of experiments with a deuteron energy of 1 to 5GeV/nucleon and protons with energy of 1 to 10 GeV of basic first direction - the integral data.

2. Experimental

2.1. The Quinta assembly

A new "ready to use" assembly Quinta, located at the Joint Institute for Nuclear Research (JINR), Dubna, Russia, has been available for the E&T RAW collaboration since the end of the year 2009. It is an assembly massive uranium target and lead shielding (refer to Fig 1). The Quinta assembly, consists of a total of 512 kg of natural uranium. It is composed of five

sections, each being 114 mm long and separated by a 17 mm air gap which allows the placement of samples mounted onto special plates (refer to Fig. 1 and Fig. 3). The uranium exists as many cylindrical rods, where each rod is 36 mm in diameter, 104 mm in length and 1.72 kg in mass. These dimensions are inclusive of a 1 mm thick impervious outer aluminum casing which is present for safety reasons. Excluding the first section, 61 rods are arranged in a hexagonal lattice with a pitch size of 36 mm and enclosed in a hexagonal aluminum container with a wall thickness of 5 mm. The first section contains only 54 rods and the removal of the central 7 rods is to create a beam window. This beam window is 80 mm in diameter and serves to reduce the loss of backward emitted/scattered neutrons. The front and back of each section are then bounded by additional aluminum plates 350 x 350 x 5 mm.

The entire uranium target-blanket reaches 638 mm in length and a mass of 538 kg including all construction materials. The five sections are mounted onto a single slab of aluminum with thickness 25 mm and surrounded by lead bricks 100 mm thick on all six sides of total weight 1780 kg. This serves as a neutron reflector and to some extent as a biological shielding for γ-rays. The top section of the lead is further supported by 16 mm of aluminum. The front of the lead castle has a square window 150 x 150 mm. Sample plates can be inserted and removed quickly into the air gaps between the sections, as well as on the front and back of the target by the presence of slots and lids located on the roof of the lead castle. The sample plates are labelled 0–5, starting from the direction of the incident beam (as shown in Fig. 3) and will be referred to accordingly throughout this text.

2.2. Irradiation details

The Quinta target was irradiated with a pulsed deuteron beam of energy 4 GeV in March 2011 and also of energy 4 GeV in December extracted from the Nuclotron accelerator, also located at the JINR. In case of the experiment session in March 2011 the Quinta assembly was not shielded with lead as presented in Fig. 1 on the left side while in the case of experiment session in December 2011 the Quinta assembly was shielded with lead as in Fig. 1 on the right side. Total number of deuterons of the irradiation is equal to 1.41(7) 10^{13} during the time of irradiation equal to 18h 30 min. But the irradiation period of December lasted approximately 17.5 h for the 4 GeV irradiations. Further details of the irradiation may be seen in Table 1. Prior to the irradiation, several polaroid films were placed on the front of Quinta to ensure the deuteron beam was striking in the centre of the beam window. In order to prevent incident beam deuterons from travelling straight through the target in the gaps between the uranium rods, the target was rotated 2^o relative to the beam axis on the x–z plane.

Table 1

Details of the three Quinta irradiations performed at the Nuclotron accelerator. Xc and Yc refer to the coordinates of the beam centre on the x–y plane.

	Experimental session in March 2011without lead shielding.	Experimental session in December 2011 shielded with lead
Incident ion	Deuteron	
Ion energy	4 GeV	4GeV
Irradiation duration	18,5 h	17.5 h
Deuterons on target	1.41(7)x10^{13}	1.94(5) 10^{13}
X_c (cm)	1.2 ± 0.2	1.4 ± 0.2
Y_c (cm)	-0.7 ± 0.2	0.2 ± 0.2
$FWHM_x$ (cm)	2.2 ± 0.3	1.5 ± 0.3
$FWHM_y$ (cm)	2.3 ± 0.3	1.4 ± 0.3

2.2.1. Measurement of beam fluence and position.

The total number of deuterons to hit the Quinta target was determined by the activation of aluminium via beam induced $^{27}Al(d,3p2n)^{24}Na$ reactions. The complete experimental methodology and results detailing the determination of the deuteron beam fluence, beam position and shape has been published previously [2]. Nevertheless, for completeness, a brief summary from [2] is provided in the following paragraph. Three independent aluminium foil monitors were placed between the beam output and the front of the Quinta target. The three monitors were placed between 2 and 3 m away from the Quinta target to avoid backscattered neutrons contaminating the measurement. Only three experimental values for the $^{27}Al(d,3p2n)^{24}Na$ cross section in the GeV range at 2.33 [3], 6.0 and 7.3 GeV ([4] are known. Therefore, the cross section at 2, 4 and GeV energies were estimated from interpolating the curve fitted to experimental data in the energy range of 0.1–7.3 GeV. The $^{27}Al(d,3p2n)^{24}Na$ cross section was found to be 15.4 ± 1.5 mb, 14.5 ± 1.5 mb, and 14.0 ± 1.4 for 2, 4 and 6 GeV deuterons, respectively and 16.4 ± 1.6 mb and 14.5 ± 1.5 mb for 1 and 4 GeV deuterons, respectively. The three foils were each analyzed independently by different groups and good agreement between all three measurements was reached. The weighted mean value of the total number of deuterons on the Quinta target was found to be 1.69(8) 10^{13}, 1.41(7) 10^{13} and 1.91(10) 10^{13} for the 2 , 4 and 6 GeV irradiations, respectively and 1.50(4) 10^{13} and 1.94(5) 10^{13} for the 1 and 4 GeV irradiations, respectively.

The beam position and beam shape was determined using two separate techniques. The first involved measuring the yield of reaction products produced by beam induced reactions on natural copper foils (method described in [5]). The other method utilized an array of fission track detectors measuring beam induced $_{nat}Pb(d,f)$ reactions [6]. Both the copper activation foils and fission track detectors were placed directly in front of the Quinta target on the surface of the lead castle. The beam shape was fitted to a Gaussian and the resulting FWHM in the vertical and horizontal directions, as well as the positioning of the beam centre is presented in Table 1.

2.3. Activation analysis of yttrium samples.

A total of twelveYttrium-89 activation foils (purity > 99.99%) were placed in the Quinta target on the detector plates in front of, between the five sections, and on the rear of the target in two positions at varying radial distances (4 and 8 cm; see Fig. 2) from the deuteron beam axis for each irradiations. The dimensions of Quinta assembly and location of yttrium foils are presented in Fig. 2.

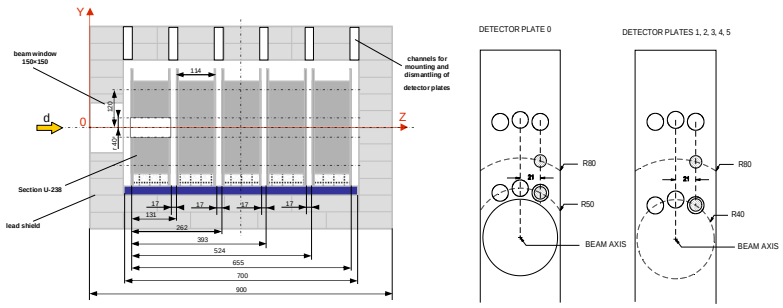

Figure 2. Dimensions of Quinta assembly and location of yttrium foils. On the left there is a longitudinal view of the assembly, on the right there are yttrium foils locations on the detector plates.

Two types of samples were used: samples which were made of solid yttrium foil with dimensions 25 × 25 × 0.64 mm3, with weight ~ 1.8 g and samples which had form of pills made of compressed yttrium powder with dimensions diameter 9 × 1.5 mm^3, with weight ~ 0.6 − 0.8 g.

The Yttrium-89 detectors have following advantages: one stable isotope - Y89, several threshold reaction channels, several resulting isotopes with long enough half life time – longer than 12 hours. First threshold energy of the reaction (n, 2n) giving ^{88}Y is possible for the energy of neutrons equal 11.5 MeV. The next threshold energies 20.8, 32.7, 42.1 and 54.4 MeV are for the reactions (n, 3n) ^{87}Y, (n, 4n) ^{86}Y, (n, 5n) ^{85}Y and (n, 6n) ^{84}Y respectively. The isotopes detected in the yttrium samples are listed in Table 2

Table 2. ^{89}Y neutron-induced reactions, threshold energies (MeV), half lives, used γ-lines (keV)and theirs intensity.

Reaction	Threshold energy [MeV]	Half-life	Used γ-line [keV]	Intensity of used γ-line [%]
^{89}Y (n,γ) ^{90m}Y	0	3.19 h	202.5	97.3
			479.2	90.7
^{89}Y (n,2n) ^{88}Y	11.6	106.65 d	898.0	93.7
			1836.1	99.2
^{89}Y (n,3n) ^{87}Y	21.1	79.8 h	388.5	82
			484.8	89.7
^{89}Y (n,3n) ^{87m}Y	21.6	13.37 h	380.8	78
^{89}Y (n,4n) ^{86}Y	33.0	14.74 h	627.7	32.6
			703.3	15.4
			777.4	22.4
			1076.6	82
			1153.0	30.5
			1854.4	17.2
			1920.7	20.8
^{89}Y (n,4n) ^{86m}Y	33.2	48 m	208.1	94
^{89}Y (n,5n) ^{85}Y	42.6	2.68 h	231.7	84
			504.5	60
			913.9	9

After irradiation, the samples were removed and transported away to be analyzed with gamma spectrometry. All 12 samples were measured using a HPGe n-type coaxial detector, manufactured by CANBERRA Industries. Measurements began ~1.5 h after irradiation had stopped, continuing for up to 6 days afterwards. The spectra collection times ranged from 15 min to just over 3 h. All spectra were analyzed using the DEIMOS [7] program.. Using this program one performed the gamma line energy calibrations, and determined line absolute intensity and half width of the line (FWHM - Full Width at Half Maximum) and respective errors. Finally we calibrate all the results to B parameters by the below calibration formula.

$$B = N_1 \cdot \frac{1}{m \cdot I} \cdot \frac{\Delta S(G) \cdot \Delta D(E)}{\frac{N_{abs}}{100} \cdot \varepsilon_p(E) \cdot COI(E,G)} \cdot \frac{(\lambda \cdot t_{ira})}{[1 - \exp(-\lambda \cdot t_{ira})]} \cdot \exp(\lambda \cdot t_+) \cdot \frac{\frac{t_{real}}{t_{live}}}{[1 - \exp(-\lambda \cdot t_{real})]} \quad (1)$$

where B number of nuclei per gram of a sample material and per one primary deuteron
N_1 peak (line) area
N_{abs} the absolute intensity of given line in percent [%]

$\varepsilon_p(E)$ detector efficiency function of energy (polynomial)
COI(E,G) cascade effect coefficient function of energy and geometry
$\Delta S(G)$, $\Delta S(G)$ calibrations function for thickness and shape of detectors
I total number of primary protons
$t_{1/2}$ half life time
t_{ira} elapsed time of irradiation
t_+ elapsed time from the end of irradiation to the beginning of measurement
t_{real} elapsed time of the measurement
t_{live} "live" time of measurement
m mass of the sample (target) in grams

Spatial distributions of ^{88}Y, ^{87}Y, ^{86}Y and ^{85}Y isotope production for the deuteron beam of 2.0, 4.0 and 6.0 (March 2011) GeV and 1 and 4 GeV (December 2011)in the Quinta assembly were measured. The error of spatial distributions of ^{88}Y, ^{87}Y, ^{86}Y, ^{85}Y isotope production are from 7E-08 to 1E-06 (it depends of the point). Since we are interested to compare the experimental results for the deuteron beam of 4 GeV of the both experimental sessions you can find the spatial distribution of ^{88}Y, ^{87}Y, ^{86}Y and ^{85}Y isotope production in Table 3a and Table 3b of the sessions.

Table 3a. Isotope production per one gram of ^{89}Y detector and per deuteron of energy equal to 4 GeV of the March session (without lead shielding).

Residual nuclei $T_{1/2}$, γ – lines used	**Radial distance Cm**	**Radial distance from front of U target , cm**					
		0	**1(13.1)**	**2(26.2)**	**3(39.3)**	**4(52.4)**	**5(65.5)**
^{89}Y(n,2n)^{88}Y-11.5 MeV $T_{1/2}$=106.65 d, Eγ=898.0, 1836.0 keV	4.0	3,08E-06	2,37E-05	8,16E-05	3,15E-05	1,41E-05	5,04E-06
	8.0	1,90E-06	1,09E-05	1,96E-05	1,55E-05	6,98E-06	2,96E-06
^{89}Y(n,3n)^{87}Y-20.8 MeV $T_{1/2}$ =3.32 d Eγ=388.5, 484.8 Kev	4.0	1,40E-06	7,98E-06	3,90E-05	1,47E-05	6,79E-06	2,76E-06
	8.0	9,17E-07	4,79E-06	1,08E-05	8,66E-06	4,44E-06	2,06E-06
^{89}Y(n,4n)^{86}Y-32.7 MeV $T_{1/2}$ =0.614 d Eγ=1076.0 keV	4.0	2,88E-07	2,29E-06	1,47E-05	5,38E-06	2,37E-06	1,09E-06
	8.0	2,32E-07	1,20E-06	2,90E-06	2,56E-06	1,21E-06	5,80E-07
^{89}Y(n,5n)^{85}Y-42.1 MeV $T_{1/2}$ = 2.86h Eγ= keV	4.0	7,83E-08	6,00E-07	5,09E-06	1,69E-06	8,15E-07	3,55E-07
	8.0	7,86E-08	3,42E-07	9,32E-07	9,37E-07	4,37E-07	2,53E-07

All the results we present in 3D graphs. An example of the isotope production Y-88 presented in Figs. 3a and 3b show that the Y-88 isotope production have maximum of axial distribution in the position of about 13 cm along the target for both experimental sessions with and without lead shielding of the QUINTA uranium target..

The general feature of the experimental spatial distribution of ^{88}Y, ^{87}Y, ^{86}Y and ^{85}Y isotopes production for the deuteron beam of 4.0 in the Quinta setup is that the maximum yield is at about 13 cm from the front of the U-238 spallation target and that the yield is decreasing with increasing radial distance from the target axis.

Table 3b. Isotope production per one gram of ^{89}Y detector and per deuteron of energy equal to 4 GeV of the December session (with lead shielding).

Residual nuclei $T_{1/2}$, γ – lines used	**Radial distance Cm**	**Radial distance from front of U target , cm**					
		0	**1(13.1)**	**2(26.2)**	**3(39.3)**	**4(52.4)**	**5(65.5)**
^{89}Y(n,2n)^{88}Y-11.5 MeV $T_{1/2}$=106.65 d, Eγ=898.0, 1836.0 keV	4.0	3,24E-06	2,49E-05	4,66E-05	2,77E-05	1,39E-05	6,43E-06
	8.0	1,99E-06	1,05E-05	2,03E-05	1,34E-05	7,39E-06	3,85E-06
^{89}Y(n,3n)^{87}Y-20.8 MeV $T_{1/2}$ =3.32 d Eγ=388.5, 484.8 Kev	4.0	1,34E-06	9,61E-06	2,23E-05	1,34E-05	6,88E-06	3,32E-06
	8.0	7,49E-07	4,05E-06	2,23E-05	6,63E-06	3,79E-06	2,05E-06
^{89}Y(n,4n)^{86}Y-32.7 MeV $T_{1/2}$ =0.614 d Eγ=1076.0 keV	4.0	3,65E-07	3,23E-06	7,86E-06	5,57E-06	2,84E-06	1,34E-06
	8.0	2,20E-07	1,25E-06	7,86E-06	2,46E-06	1,43E-06	8,01E-07
^{89}Y(n,5n)^{85}Y-42.1 MeV $T_{1/2}$ = 2.86h Eγ= keV	4.0	1,53E-07	0,0E+00	3,73E-06	2,86E-06	1,39E-06	6,91E-07
	8.0	9,12E-08	4,81E-07	1,64E-06	1,17E-06	6,78E-07	4,06E-07

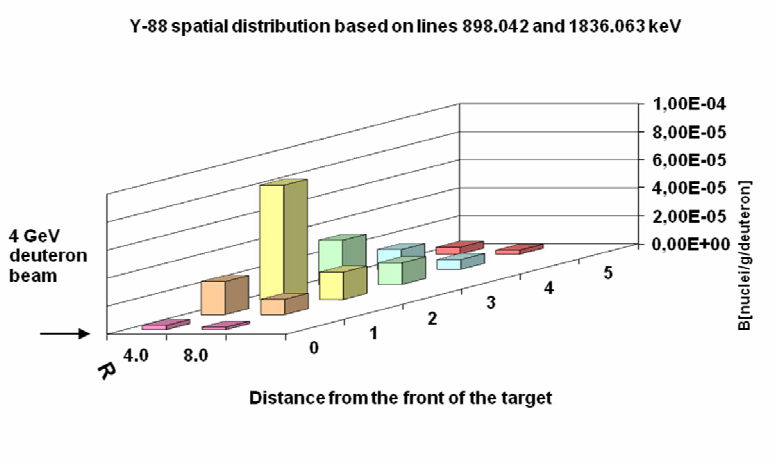

Fig. 3a. Spatial distribution (radial & axial) of Y88 production for the deuteron beam 4GeV in the first experimental session (March 2011) when the uranium target was not lead shielded.

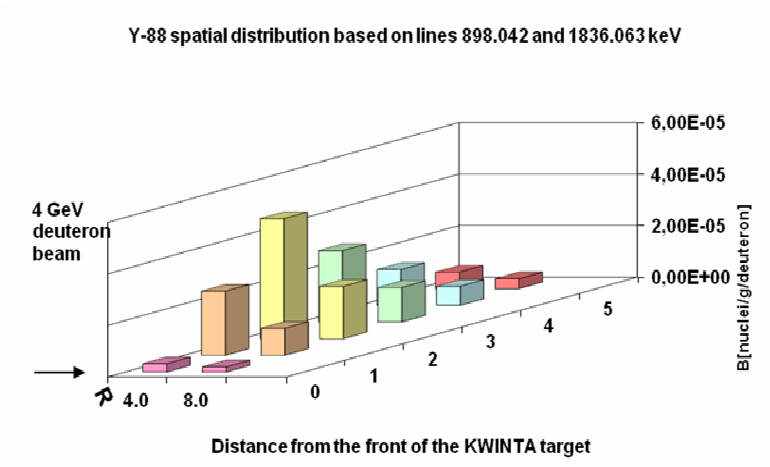

Fig. 3b. Spatial distribution (radial & axial) of Y88 production for the deuteron beam 4GeV in the second experimental session (December 2011) when the uranium target was lead shielded.

3. Evaluation of average high energy neutron flux in the Yttrium-89 detectors location inside the U/Pb assembly.

Precise assign of the neutron flux in the location of yttrium detector is not possible having only four experimental data of Y-88, Y-87, Y-86 and Y-85 isotopes produced in (n,xn) reactions at our disposal. Since in the earlier experiments we were able to detect only three produced isotopes Y-88, Y-87 and Y-86 so we have limited our analysis of evaluation the average high neutron flux inside the Quinta assembly also to the three isotopes in order to make easier comparison between them.

Having already determined isotope production per one gram of sample and per one beam deuteron at specified positions of the Quinta setup for the three isotopes Y-88, Y-87 and Y-86 we can evaluate three average high energy neutron fluxes in each Yttrium -89 detectors location for certain energy ranges. The energy ranges is roughly determined by the microscopic cross section in function of energy for the (n,xn) reactions of the three isotopes ^{88}Y, ^{87}Y and ^{86}Y. The following three threshold energy 11.5, 20.8 and 32.7MeV for the reactions ^{89}Y(n, 2n)^{88}Y, ^{89}Y (n, 3n)^{87}Y and ^{89}Y(n,4n) ^{86}Y appoint the first two energy ranges (11.5 - 20.8 MeV) and (20.8 - 32.7MeV) of the neutron fluxes $\overline{\phi_1}$ and $\overline{\phi_2}$. The third energy range begins at the energy 32.7MeV and ends when the microscopic cross section is comparatively low with the maximum cross section of . ^{89}Y(n,4n) ^{86}Y reaction where is evaluated the neutron flux $\overline{\phi_3}$.

As we have obtained spatial distribution of Y-88, Y-87 and Y-86 isotopes production from (n,xn) reactions, so we also obtain the spatial distribution of high neutron flux for the three energy ranges inside the Quinta setup.

3.1. Assignation of the microscope cross section for the (n,xn) reaction of ^{89}Y

To calculate the high energy neutron field we need to know the microscopic cross section for the ^{89}Y-(n,xn) reactions. Some cross section data for neutron induced reactions were retrieved from the literature [8, 9] and some cross sections were calculated using the TALYS code [10, 11] because the experimental nuclear data libraries are poor for the Yttrium-89 isotope. No neutron induced reaction cross section for reaction ^{89}Y(n,4n) were found in the EXFOR data base or open literature. Only the data for the cross section of ^{89}Y(n, 2n) and several points of ^{89}Y(n, 3n)^{87}Y reactions we could find [12],[13].

TALYS is a software for the simulation of nuclear reactions. Many state-of-the-art nuclear models are included to cover all main reaction mechanisms encountered in light particle-induced nuclear reactions. TALYS provides a complete description of all reaction channels and observables, and is user-friendly. TALYS is a versatile tool to analyse basic microscopic experiments and to generate nuclear data for applications. It calculates total and partial cross-sections, energy spectra, angular distributions, double-differential spectra, residual production cross sections, and recoils. It has been tested with experimental data with very good results.

The TALYS code was used to generate microscopic cross sections for several ^{89}Y(n, xn) reactions. Comparison of experimental microscopic cross sections of the reaction ^{89}Y(n, 2n)^{88}Y and the reaction ^{89}Y(n, 3n)^{87}Y with the generated microscopic cross sections for the two reactions shows very good agreement. This gives us confidence in the calculated cross sections by TALYS code of the ^{89}Y (n, 3n)^{87}Y and ^{89}Y(n, 4n)^{86}Y reactions.

3.2. Derivation of the average neutron flux formula.

In general the number of yttrium isotopes (N_y) in the yttrium 89 detector of volume V_p in the chosen energy range can be expressed:

$$N_y = V_p \, \bar{\phi} \, N \, \bar{\sigma} \, t, \qquad (1)$$

where

$\overline{\Phi}$ - average neutron flux in the chosen energy range [n/cm^2·s]

$$\overline{\Phi} = (E_2 - E_1)\,\overline{\psi}\ ;\ \overline{\psi} = \frac{\int_{E_1}^{E_2} \psi(E)\,dE}{E_2 - E_1}$$

$\psi(E)$ – neutron flux density [n/cm^2·s·MeV]

N – number of yttrium 89 isotopes in volume unit [cm^{-3}]

$\overline{\sigma}$ -average microscopic cross section for the reaction (n, xn) in the energy range (E_1 – E_2) [barns],

$$\overline{\sigma} = \frac{\int_{E_1}^{E_2} \sigma(E)dE}{E_2 - E_1}$$

σ - microscopic cross section for the reaction (n, xn)

t -deuteron irradiation time.

$$N = \frac{\rho_p}{G^{89}} A \qquad (2)$$

where

ρ_p - specific weight of Y^{89},

G^{89} - gram-atom of Y^{89},

A - Avogadro's number,

We assume that the average neutron flux in the chosen energy range ($\overline{\Phi}$) is constant versus time during deuteron irradiation.

From the other side the number N_y of Y-88, Y-87 and Y-86 isotopes produced in (n,xn) reactions in the detector we can obtain as:

$$N_y = B^y\, W_p\, S\ , \qquad (3)$$

Where

B^y – isotope production per one gram of sample and per one beam deuteron,

W_p – weight of detector; $W_p = \rho_p V_p$,

S - total number of deuterons.

Combining the equation (1) with the equation (3) we obtain:

$$\overline{\phi} = \frac{B^y\, S\, G^{89}}{\overline{\sigma}\, A\, t} \text{ [1/cm}^2\text{·s]} \qquad (4)$$

The above equation (4) pertains only to one assumed isotope. When we consider three isotopes then we have to solve three equations. First of all we have to define the three energy ranges for the three average neutron fluxes which are of our interest. In Fig. 4 the three energy ranges for the three average neutron fluxes which are of our interest are presented.

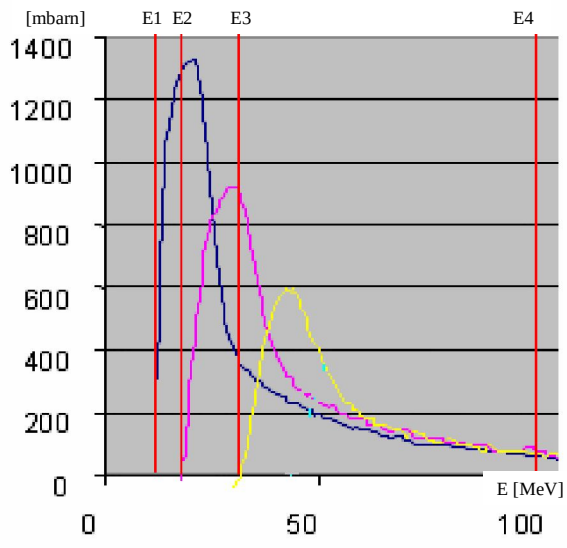

Fig.4. Microscopic cross sections for ^{89}Y(n, 2n)^{88}Y, ^{89}Y (n, 3n)^{87}Y and ^{89}Y(n,4n) ^{86}Y reactions generated by TALYS code and three energy ranges for the three average neutron fluxes which are of our interest.

By choosing the first three threshold energies E1=11.5 MeV, E2=20.8 MeV and E3=32.7 MeV for the reactions ^{89}Y(n, 2n)^{88}Y, ^{89}Y (n, 3n)^{87}Y and ^{89}Y(n,4n) ^{86}Y and the fourth E4=100 MeV when the microscopic cross section is comparatively low with the maximum cross section of . ^{89}Y(n,4n) ^{86}Y reaction we have defined the three average neutron fluxes $\overline{\phi_1}$, $\overline{\phi_2}$, $\overline{\phi_3}$ which are of our interest. These assumptions enabled us to write the following three algebraic equations:

$$B^{88}\, C = \overline{\phi}_1\, \overline{\sigma}_{11} + \overline{\phi}_2\, \overline{\sigma}_{12} + \overline{\phi}_3\, \overline{\sigma}_{13} \quad (5)$$

$$B^{87}\, C = 0 + \overline{\phi}_2\, \overline{\sigma}_{22} + \overline{\phi}_3\, \overline{\sigma}_{23} \quad (6)$$

$$B^{86}\, C = 0 + 0 + \overline{\phi}_3\, \overline{\sigma}_{33} \quad (7)$$

where

B^{88},·B^{87},·B^{86} - measured isotopes of ^{88}Y, ^{87}Y and ^{86}Y respectively per one gram of detector and per one beam deuteron

$$C = \frac{S\, G^{89}}{A\, t}$$

$\overline{\sigma_{11}}$. – .$\overline{\sigma_{33}}$ - microscopic cross section of the measured isotopes for the reaction (n, xn) in the three chosen energy ranges,

$\overline{\phi_1} - \overline{\phi_3}$ - unknown average neutron fluxes in the three chosen energy ranges.

Solution of the above three equations let us to evaluate the average neutron fluxes in the three energy ranges expressed in [n/cm^2·s]:

$$\overline{\phi_1} = \frac{C}{\overline{\sigma_{11}}}[B^{88} - B^{87}\frac{\overline{\sigma_{12}}}{\overline{\sigma_{22}}} + B^{86}(\frac{\overline{\sigma_{23}}\,\overline{\sigma_{12}}}{\overline{\sigma_{33}}\,\overline{\sigma_{22}}} - \frac{\overline{\sigma_{13}}}{\overline{\sigma_{33}}})] \quad (8)$$

$$\overline{\phi_2} = \frac{C}{\overline{\sigma_{22}}}[B^{87} - B^{86}\frac{\overline{\sigma_{23}}}{\overline{\sigma_{33}}}] \quad (9)$$

$$\overline{\phi_3} = \frac{C}{\overline{\sigma_{33}}}B^{86} \quad (10)$$

Number of measured isotopes in the detector assigns the number of algebraic equations what in turn assigns the number of unknown neutron fluxes in the chosen neutron energy ranges which are possible to be evaluated. The more of measured isotopes in the detector the more precise evaluation of the high energy neutron spectrum is obtained.

3.3 Evaluated high energy neutron fields in the chosen three energy ranges.

Using the microscopic cross sections for the reactions ^{89}Y(n, 2n), (n, 3n) and (n,4n) generated by TALYS code and the experimental data (parameter B) we have evaluated the average high energy neutron flux in the yttrium 89 detectors located inside the Quinta assembly for the three energy ranges (11.5 - 20.8 MeV), (20.8 - 32.7MeV) and (32.7 – 100 MeV).

The following average microscopic cross sections for the reactions ^{89}Y(n, 2n)^{88}Y, ^{89}Y (n, 3n)^{87}Y and ^{89}Y(n,4n) ^{86}Y in the three chosen energy ranges are used to make calculations using the formulas (8), (9) and (10):

$\overline{\sigma_{11}}$ =1,03 E-24 cm^2 for ^{89}Y(n, 2n)^{88}Y reaction in the energy range 11,5-20,8 MeV

$\overline{\sigma_{12}}$ =7,33E-25 cm^2 for ^{89}Y(n, 2n)^{88}Y reaction in the energy range 20,8-32,7 MeV

$\overline{\sigma_{13}}$ =1,50E-25 cm^2 for ^{89}Y(n, 2n)^{88}Y reaction in the energy range 32,7-100 MeV

$\overline{\sigma_{22}}$ =5,69E-25 cm^2 for ^{89}Y (n, 3n)^{87}Y reaction in the energy range 20,8-32,7 MeV

$\overline{\sigma_{23}}$ =2,88E-25 cm^2 for ^{89}Y (n, 3n)^{87}Y reaction in the energy range 32,7-100 MeV

$\overline{\sigma_{33}}$ =2,52E-25 cm^2 for ^{89}Y(n,4n) ^{86}Y reaction in the energy range 32,7-100 MeV

Comparisons of average neutron flux densities and average neutron flux densities per deuteron and their energy for the three neutron energy ranges(11,5-20,8 MeV, 20,8-32,7 MeV, 32,7-100 MeV) and for the deuteron beam energy equal to 4 GeV of both experiments (in March and December 2011) were performed.

The average neutron flux densities for both experiments are presented below in Figs 5a, 5b, 5c, 5d, 5e and 5f.

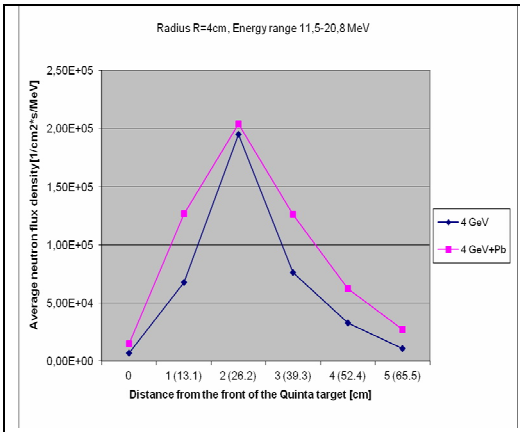

Fig. 5a. Average neutron flux densities in the Quinta uranium target at 4 cm radius enfolded with lead reflector and without it in the range of 11,5-20,8 MeV irradiated with deuterons of energy 4 GeV.

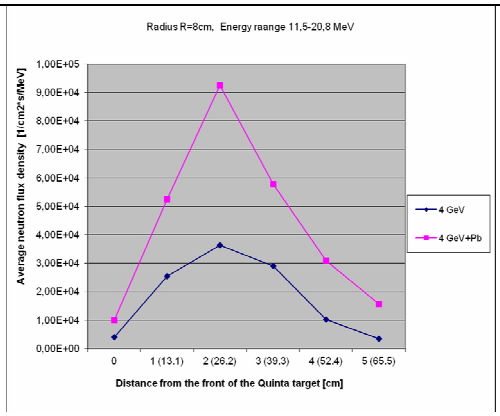

Fig. 5b. Average neutron flux densities in the Quinta uranium target at 8 cm radius enfolded with lead reflector and without it in the range of 11,5-20,8 MeV irradiated with deuterons of energy 4 GeV.

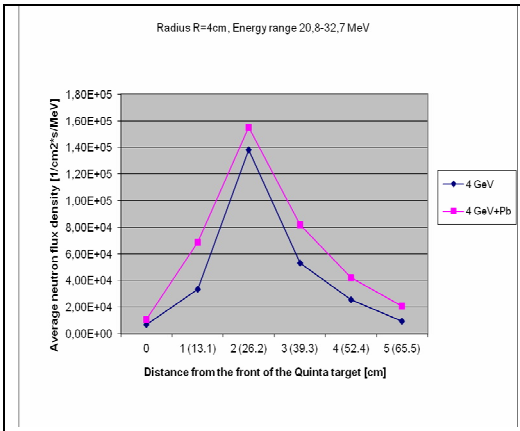

Fig. 5c. Average neutron flux densities in the Quinta uranium target at 4 cm radius enfolded with lead reflector and without it in the range of 20,8-32,7 MeV irradiated with deuterons of energy 4 GeV.

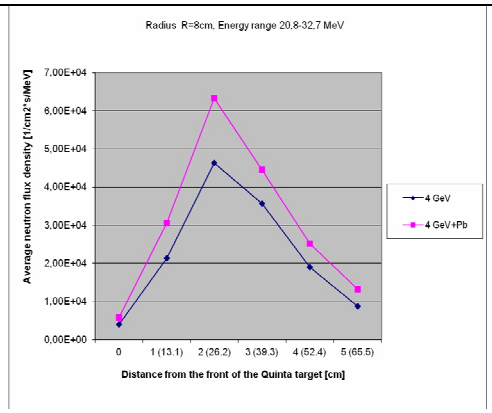

Fig. 5d. Average neutron flux densities in the Quinta uranium target at 8 cm radius enfolded with lead reflector and without it in the range of 20,8-32,7 MeV irradiated with deuterons of energy 4 GeV.

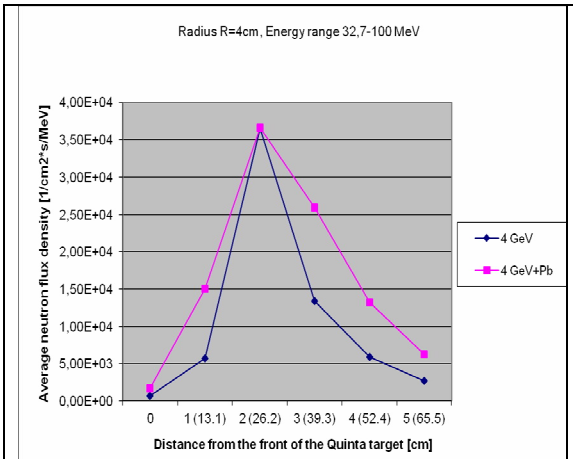

Fig. 5e. Average neutron flux densities in the Quinta uranium target at 4 cm radius enfolded with lead reflector and without it in the range of 32,7-100 MeV irradiated with deuterons of energy 4 GeV.

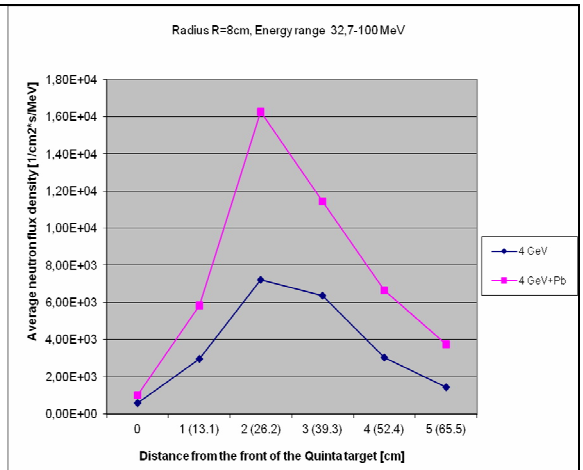

Fig. 5f. Average neutron flux densities in the Quinta uranium target at 8 cm radius enfolded with lead reflector and without it in the range of 32,7-100 MeV irradiated with deuterons of energy 4 GeV.

Since the curves of the neutron flux densities nearly overlap at the radius 4 cm in the area close to the spallation uranium target for both of the experiments with and without the lead shielding we can assume that the irradiation conditions were alike (see Figs 5a, 5c and 5e).

Table 4. Neutron densities increase in the volume of QUINTA uranium target caused by the lead reflector (shielding) in the case of 4 GeV deuteron irradiation.

Energy range [MeV]	Radious [cm]	Neutron density in maximum point (without lead shield – March 2011) [1/cm^2·s/MeV]	Neutron density in maximum point (with lead shield –December 2011) [1/cm^2·s/MeV]	Neutron density increase in the volume of QUINTA uranium target.
11,5-20,8	4 8	$1.95\ 10^5$ $3.64\ 10^4$	$2.04\ 10^5$ $9.25\ 10^4$	1.045 2.54
20,8-32,7	4 8	$1.82\ 10^5$ $4.63\ 10^4$	$1.55\ 10^5$ $6.33\ 10^4$	0.85 1.37
32,7-100	4 8	$3.65\ 10^4$ $7.20\ 10^3$	$3.66\ 10^4$ $1.63\ 10^4$	1.002 2.26

The measurement show that the neutron flux density increases in whole volume of the QUINTA assembly due to the lead shielding (see Figs 5a -5f). The lead shielding influence on the neutron spectra is more pronounced in the volume located closer to the shielding. This is clearly seen comparing the neutron flux densities distribution along the uranium target axis of the two experimental sessions for the same deuteron beam energy of 4 GeV with and without the lead shielding. In the separate energy ranges the neutron flux densities increases over 2 times but in the neutron range 20.8 – 32.7, which is only about 1.4 times (see Figs 5a – 5f and Table 4). Due to this increase the neutron flux distribution is more equal in the whole volume of the QUINTA assembly. This let us to infer that the layout of QUINTA assembly which is a deep subcritical nuclear core with hard neutron spectrum in a big volume to some extent is a suitable device for radioactive minor actinides burn-up in a big industrial scale after some innovation.

While the lead shield of the Quinta assembly causes decrease of neutron flux for the area close (4 cm) to the spallation target (especially in the position where maximum of flux occurs), inversely away from (8 cm) the spallation target it causes increase of the flux comparatively.

4. Conclusions

The general feature of the experimental spatial distribution of 88Y, 87Y, 86Y and 85Y isotopes production is that the maximum yield is at about 13 cm from the front of the U-238 spallation target and that the yield is decreasing with increasing radial distance from the target axis.

Also, the general feature of the experimental neutron flux density per deuteron in the Quinta assembly is that the maximum occurs at about 13 cm from the front of the U-238 spallation target and that it is decreasing with increasing radial distance from the target axis.

Since the curves of the neutron flux densities nearly overlap at the radius 4 cm in the area close to the spallation uranium target for both of the experiments with and without the lead shielding it is assumed that the irradiation conditions were alike.

The lead shielding influence on the neutron spectra is more pronounced in the volume located closer to the shielding

In the separate energy ranges the neutron flux densities increases over 2 times but in the neutron range 20.8 – 32.7, which is only about 1.4 times.

Due to this increase the neutron flux distribution is more equal in the whole volume of the QUINTA assembly.

This let us to infer that the layout of QUINTA assembly which is a deep subcritical nuclear core with hard neutron spectrum in a big volume to some extent is a suitable device for radioactive minor actinides burn-up in a big industrial scale after some innovation.

The main contribution to uncertainties in the experimental results are due to peak area calculation and statistical error coming from DEIMOS program [7]. Moreover there are uncertainties in the measurements involving the total number of the primary deuterons in each experiment. We estimate that the overall uncertainties of the experimental data to be in the range 15%-20%.

Acknowledgments

The author's would like to thank the staff of the Nuclotron accelerator of the Joint Institute of Nuclear Research, Dubna for providing access to the research facilities used in these experiments.

This work was carried out as part of the Strategic Project ''Safe Nuclear Power Engineering Development Technologies'' supported by The National Centre for Research and Development, Poland.

References

[1] <<E&T RAW>> Collaboration: V. Chilap, S.Tyutyunnikov, I. Adam, M. Kadykov, V. Pronskikh, , V. Wagner, O.Svoboda, M. Bielewicz, S. Kilim, A. Polanski, E. Strugalska-Gola, M. Szuta, A. Wojciechowski et al. *Study of deep subcritical electronuclear systems and feasibility of their application for energy production and radioactive waste transmutation; E1-2010-61.*

[2] W.Furman M. Bielewicz, S. Kilim, E. Strugalska-Gola, M. Szuta, A. Wojciechowski et al; **Recent results of the study of ADS with 500 kg natural uranium target assembly QUINTA irradiated by deuterons with energies from 1 to 8 GeV at JINR NUCLOTRON**; ;"XXI International Baldin Seminar on High Energy Physics Problems – *"Relativistic Nuclear Physics & Quantum"; Russia, Dubna, September 10 – 15, 2012 Proceedings of Science, , PoS (Baldin ISHEPP XXI) 086, 2013 .* www.pos.sissa.it

[3] Banaigs, J., Berger, J., Duflo, J., Goldzahl, L., Harff, O., Cottereau, M., Lefebvres, F., Quechon, H., Tardy-Joubert, P.,. *Determination de l'intensite d'un faisceau de deutons extrait d'un synchrotron et mesure des sections efficaces des reactions $^{12}C(d,p2n)^{11}C$ et $^{27}Al(d,3p2n)^{24}Na$ a 2,33 ;GeV. Nuclear Instruments and Methods 95, 1971,pp 307–311.* http://dx.doi.org/10.1016/0029-554X(71)90382-X.

[4] Kozma, P., Yanovsky; V.V.,. *Application of BaF_2 scintillator to off-line gamma ray spectroscopy. Czechoslovak Journal of Physics 40, 1990, pp 393–397.* http:/dx.doi.org/10.1007/BF01597913.

[5] Svoboda, I.O., 2011. *Experimental Study of Neutron Production and Transport for ADTT, Ph.D. Thesis. Czech Technical University in Prague.*

[6] Zhuk, I.V., Hashemi-Nezhad, S.R., Potapenko, A.S., Krivopustov, M.I., *Determination of high-energy proton beam profile using track detectors. Radiation Measurements 43, 2008, pp. S210–S214.* http://dx.doi.org/10.1016/ j.radmeas.2008.03.074, *ISSN: 13504487.*

[7] J. Frana – *Program DEIMOS32 for Gamma Ray Spectra Evaluation. Radioanal. and Nucl. Chem., V. 257, p.583, 2003.*

[8] S.Hilaire, Statistical Nuclear Reaction Modeling, DIF/DPTA/SPN/LMED, Trieste 2008

[9] Experimental Nuclear Reaction Data; EXFOR/CSISRS

[10] Koning A. J., Hilaire S., Duijvestijn M. C. TALYS: *Comprehensive Nuclear Reaction Modeling, International Conference on Nuclear Data for Science and Technology 2004, Santa Fe, New Mexico, 26th September-1st October 2004. AIP Conference Proceedings, Volume 769 (2005)1154-9,*

[11] *TALYS-1.0 :* A Nuclear reaction code. A.J. Koning, S.Hilaire, M.Duijvestijn. www.talys.eu

[12] Veeser L. R. et al.: Cross sections for (n,2n) and (n,3n) reaction above 14 MeV, Physical Review, Part C - Nuclear Physics, Vol. 16, p. 1792 (1977)